

## Electronic Supplementary Information

# Tuning Morphology, Surface, and Nanocrystallinity of Rare Earth Vanadates by One-Pot Colloidal Conversion of Hydroxycarbonates

Gabriela Guida,<sup>a</sup> Steven Huband,<sup>b</sup> Marc Walker,<sup>b</sup> Richard I. Walton,<sup>c</sup> and  
Paulo C. de Sousa Filho<sup>\*a</sup>

<sup>a</sup> Department of Inorganic Chemistry, Institute of Chemistry, University of Campinas (Unicamp), PO Box 6154, 13083-970 Campinas, SP, Brazil.  
<sup>b</sup> Departments of Physics and <sup>c</sup>Chemistry, University of Warwick, Coventry CV4 7AL, United Kingdom.

	Page
<b>1. ADDITIONAL EXPERIMENTAL DETAILS .....</b>	<b>S-1</b>
<b>1.1. Modelling of SAXS data .....</b>	<b>S-1</b>
<b>1.2. Luminescence overall quantum yields .....</b>	<b>S-2</b>
<b>2. ADDITIONAL DATA .....</b>	<b>S-4</b>
<b>2.1. Hydroxycarbonate particles prepared in water .....</b>	<b>S-4</b>
<b>2.2. Composition of hydroxycarbonate templates .....</b>	<b>S-5</b>
<b>2.3. Modelled SAXS intensities and related data .....</b>	<b>S-7</b>
<b>2.4. Additional microscopy images .....</b>	<b>S-12</b>
<b>2.5. FTIR spectra of (Y,Eu)VO<sub>4</sub> nanoparticles .....</b>	<b>S-14</b>
<b>2.6. N<sub>2</sub> adsorption isotherms .....</b>	<b>S-15</b>
<b>2.7. XRD data .....</b>	<b>S-16</b>
<b>2.8. Thermogravimetry of (Y,Eu)VO<sub>4</sub> nanoparticles .....</b>	<b>S-18</b>
<b>2.9. XPS Spectra .....</b>	<b>S-19</b>
<b>2.10. Luminescence spectra .....</b>	<b>S-21</b>
<b>2.11. Luminescence decay curves .....</b>	<b>S-22</b>
<b>2.12. Spectroscopic parameters .....</b>	<b>S-25</b>
<b>3. REFERENCES .....</b>	<b>S-27</b>

\* Corresponding author: [pcsfilho@unicamp.br](mailto:pcsfilho@unicamp.br)

## 1. ADDITIONAL EXPERIMENTAL DETAILS

### 1.1 Modelling of SAXS data

Small-angle X-ray scattering (SAXS) measurements were made using a Xenocs Xeuss 2.0 equipped with a micro-focus Cu K $\alpha$  source collimated with Scatterless slits. The scattering was measured using a Pilatus 300k detector with a pixel size of 0.172 mm x 0.172 mm. The distance between the detector and the sample was calibrated using silver behenate ( $\text{AgC}_{21}\text{H}_{43}\text{COO}$ ), giving a value of 2.481(5) m. The magnitude of the scattering vector ( $q$ ) is given by  $q=(4\pi\sin\theta)/\lambda$ , where  $2\theta$  is the angle between the incident and scattered X-rays and  $\lambda$  is the wavelength of the incident X-rays. This gave a  $q$  range for the detector of 0.004 Å $^{-1}$  and 0.16 Å $^{-1}$ . Samples were mounted in 1 mm borosilicate capillaries. An azimuthal integration of the 2D scattering profile was performed and the resulting data corrected for the absorption, sample thickness and solvent background. Finally, the scattering intensity was then rescaled to absolute intensity using glassy carbon as a standard.<sup>1</sup>

For variable temperature measurements a Linkam HFSX 350 was used and samples were heated to 90 °C at 5 °C min $^{-1}$ . Once at 90 °C, repeated 5 min measurements were collected for a total dwell time of 120 min. The scattering signal was modelled using the Irena package using a spherical model for the particles.<sup>2</sup> The radius of the sphere was allowed to have either a Gaussian or log-normal distribution, where an appropriate Porod slope was included at low  $q$  to model any agglomeration and a hard-sphere interaction model was used to account for inter-particle interactions.

## 1.2 Luminescence overall quantum yields

Luminescence overall quantum yields ( $q_{exp}$ ) are defined as ratio between absorbed photon flux and the emitted photon flux for a sample at a given wavelength. In this work,  $q_{exp}$  values of particle suspensions (25 mmol L<sup>-1</sup>) were estimated comparatively using a using a Horiba Quanta  $\varphi$  integrating sphere under UV excitation in 10 mm path quartz cuvettes. 2-Aminopyridine (10<sup>-5</sup> mol L<sup>-1</sup> in 0,1 mol L<sup>-1</sup> aqueous H<sub>2</sub>SO<sub>4</sub>) was used as an internal standard ( $q_{ST}=0.60$ ).<sup>3</sup> Suspensions in D<sub>2</sub>O were prepared by drying 1 mL of 25 mmol L<sup>-1</sup> suspensions in H<sub>2</sub>O at 60 °C for 24 h and resuspending the particles in 1 mL of D<sub>2</sub>O in an ultrasound bath. The calculation of overall quantum yields comprised measurements in an emission setup in the integrating sphere, collecting both the excitation peak ( $\lambda=280$  nm) and emission signals (250-750 nm). The absorptivity of the sample was assumed to be directly proportional to the attenuation of excitation line, so absorbed photon flux was estimated by comparing integrated intensities of excitation lines at 280 nm of sample and pure water as blank. The emitted photon flux was estimated from the integrated emission intensities. Finally, the overall quantum yields were estimated by Equation S1:

$$q_{EXP} = q_{ST} \left[ \frac{(I_{em}^X - I_{em}^0)(I_{exc}^0 - I_{exc}^{ST})}{(I_{em}^{ST} - I_{em}^0)(I_{exc}^0 - I_{exc}^X)} \right], \quad (S1)$$

where  $I_{em}$  are integrated intensities at the emission wavelengths and  $I_{exc}$  are integrated intensities at the excitation peak ( $\lambda_{exc}=280$  nm) [“X”, “0”, and “ST” superscripts refer to sample, blank, and standard, respectively]. A typical set of spectra of sample, standard and blank is shown in Fig. S1.

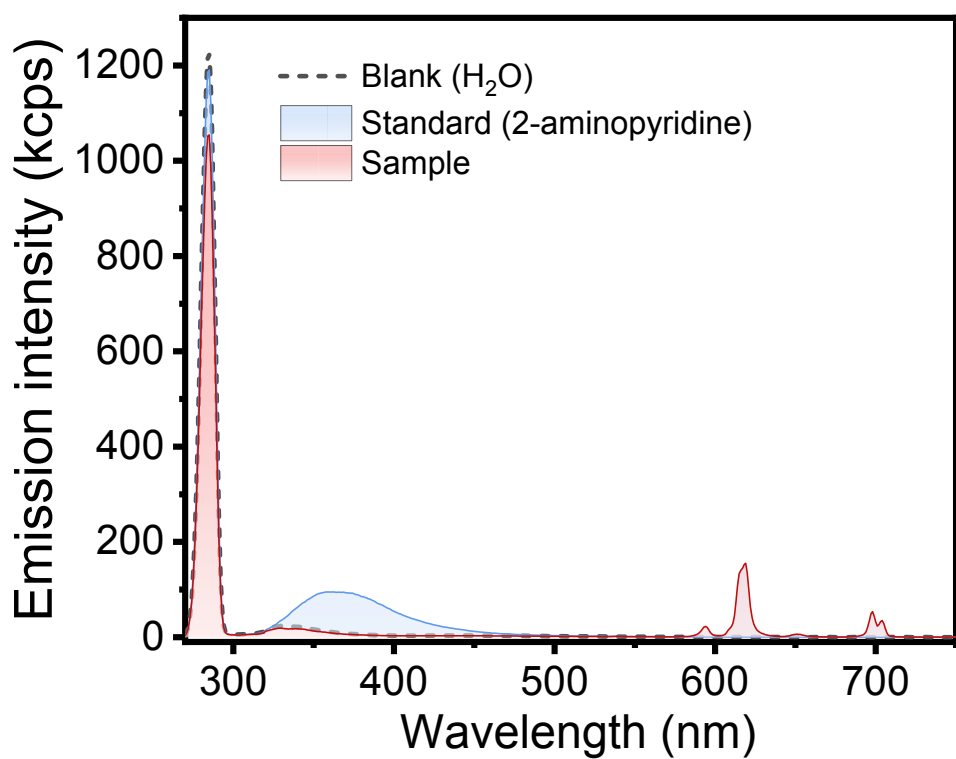


**Fig. S1.** Luminescence spectra ( $\lambda_{exc}=280$  nm) collecting both the excitation line and sample emissions for the calculation of overall quantum yields by Eq. S1: water as blank (dotted line), quantum yield standard (2-aminopyridine, blue line) and a representative sample [ $(Y_{0.80}Eu_{0.20})VO_4$  particles obtained in  $H_2O/EG=3/2$ , red line].

## 2. ADDITIONAL DATA

### 2.1 Hydroxycarbonate particles prepared in water

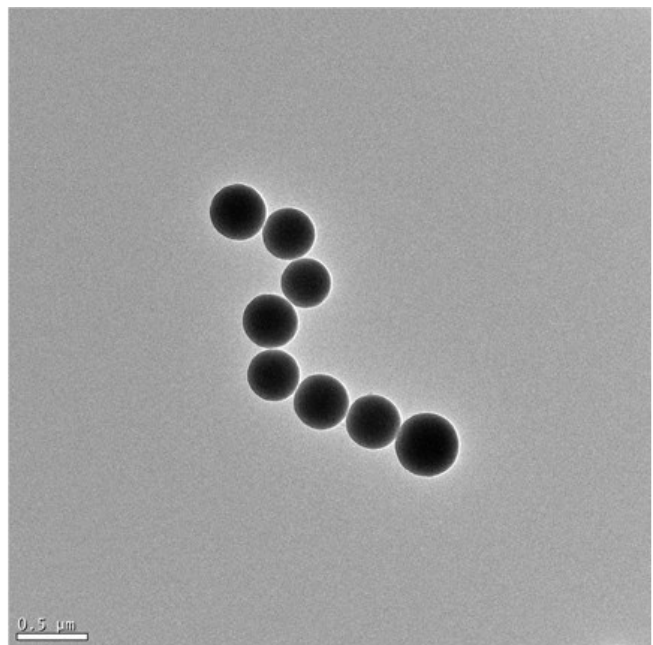
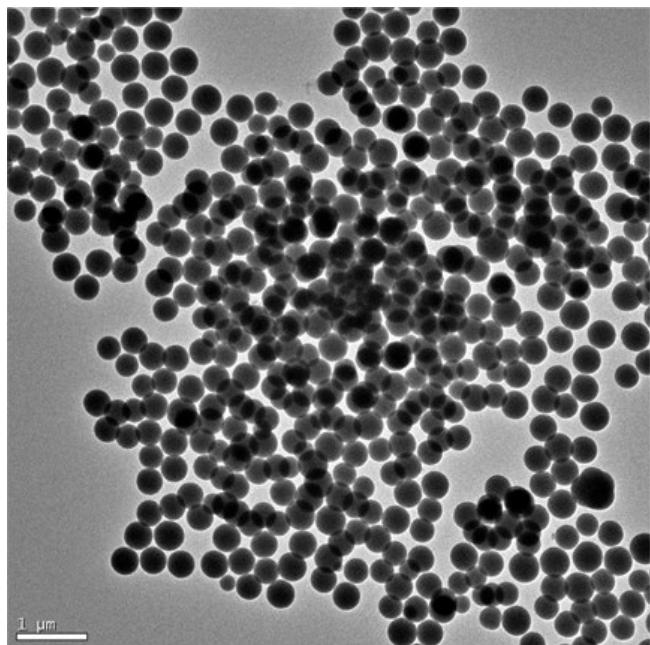


**Fig. S2.** TEM images of hydroxycarbonate particles synthesized in water via homogeneous precipitation with urea.<sup>4</sup>

## 2.2. Composition of hydroxycarbonate templates

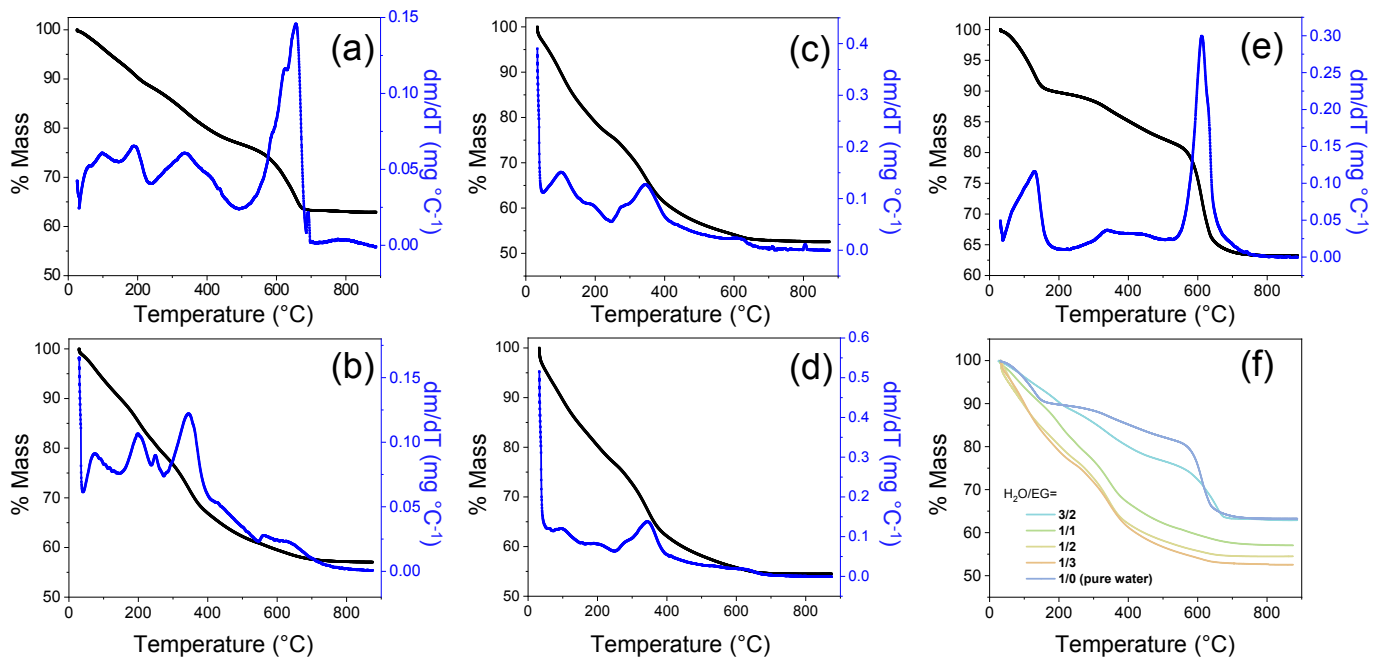


**Fig. S3.** (a-e) TGA (black lines) and DTG (blue lines) of the  $(Y_{0.95}Eu_{0.05})CO_3OH \cdot xH_2O$  nanoparticles prepared in different solvent compositions ( $H_2O/EG$  vol/vol.), namely (a)  $H_2O/EG=3/2$ , (b)  $H_2O/EG=1/1$ , (c)  $H_2O/EG=1/2$ , (d)  $H_2O/EG=1/3$ , and (e)  $H_2O/EG=1/0$  (pure water). TGA curves of the five samples are superposed in (f) for comparison.

**Table S1.** Results calculated from TGA analysis: initial mass ( $m_0$ ), weight loss in the first decomposition step ( $m_{H_2O}$ ), final residues, and calculated hydration ( $\cdot xH_2O$ ) per formula unit for the  $(Y_{0.95}Eu_{0.05})CO_3OH \cdot xH_2O$  particles prepared in different solvent compositions ( $H_2O/EG$ )

$H_2O/EG$ (vol/vol) =	$m_0$ (mg)	Weight loss (1 <sup>st</sup> step), $m_{H_2O}$ (mg)	Final residue (% $m_0$ )	Total hydration ( $\cdot xH_2O$ , $x=$ )
<b>3/2</b>	6.834	0.677	63.09	1.0
<b>1/1</b>	15.838	1.335	57.05	0.9
<b>1/2</b>	7.592	1.308	54.49	1.8
<b>1/3</b>	9.539	1.752	52.55	1.9
<b>1/0 (pure <math>H_2O</math>)</b>	6.651	0.676	63.33	1.1

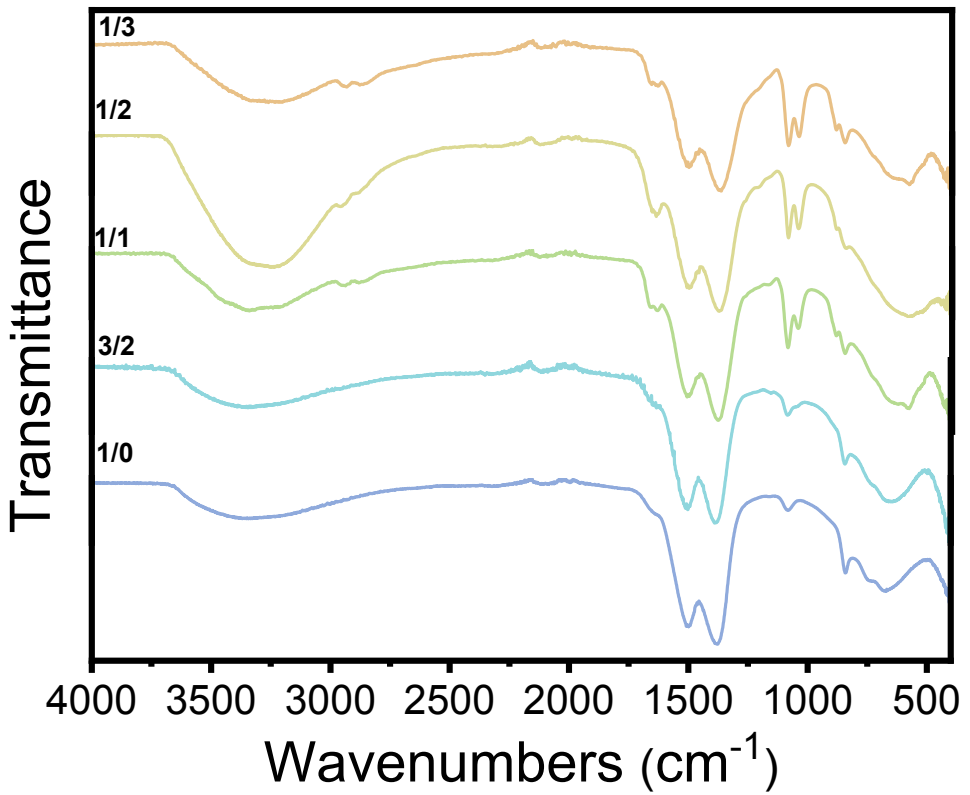


**Fig. S4.** Infrared spectra of the RE hydroxycarbonate particles  $[(Y_{0.95}Eu_{0.05})CO_3OH \cdot xH_2O]$  prepared using different H<sub>2</sub>O/EG volume ratios from 1/3 (top) to 1/0 (pure water, bottom).

### 2.3. Modelled SAXS Intensities and related data

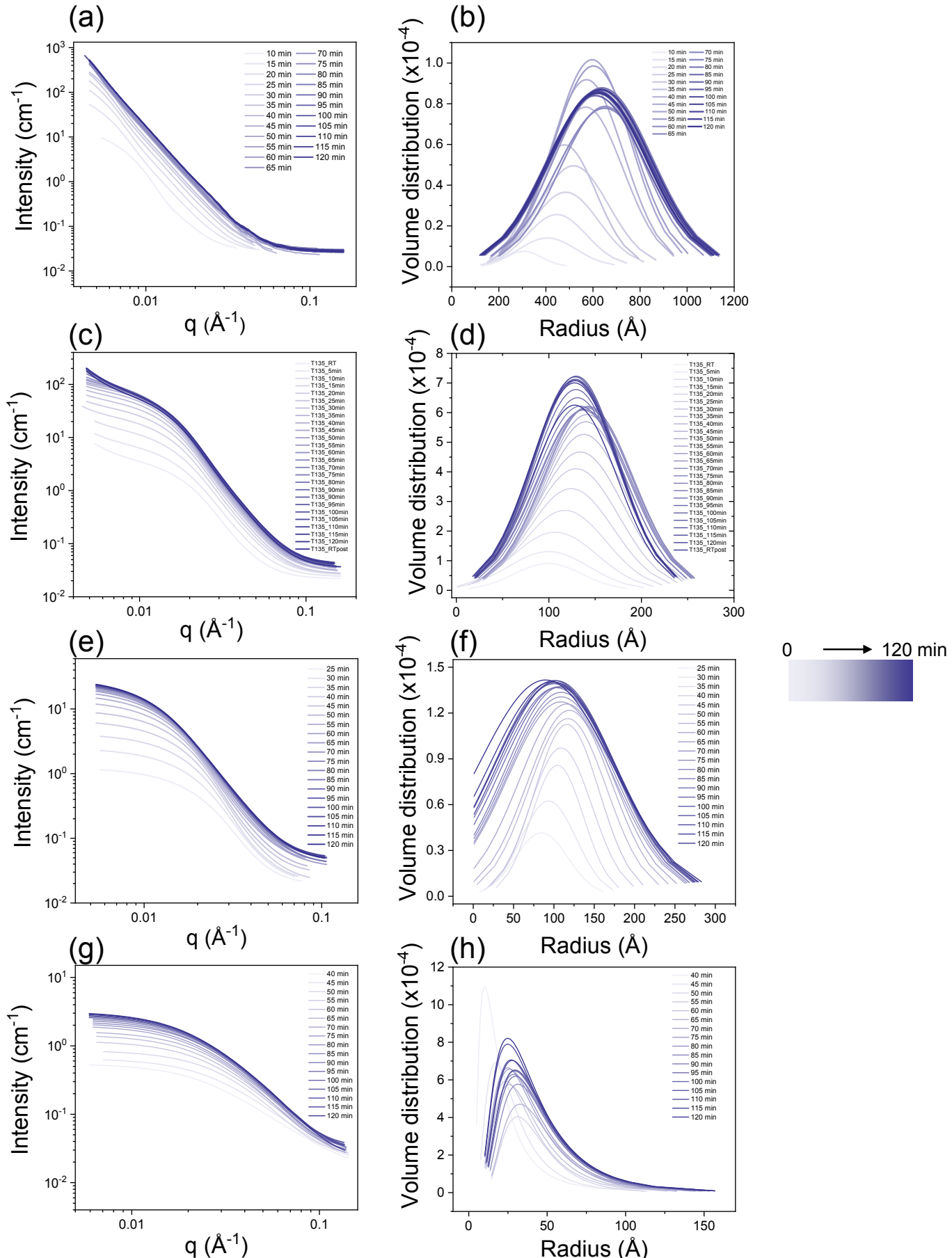


**Fig. S5.** Modelled SAXS profiles (left) and particle volume distributions (right) in different reaction times of hydroxycarbonate particles  $[(\text{Y}_{0.95}\text{Eu}_{0.05})\text{CO}_3\text{OH} \cdot x\text{H}_2\text{O}]$  prepared by precipitation with urea in different  $\text{H}_2\text{O}/\text{EG}$  ratios: (a,b) 3/2, (c,d) 1/1, (e,f) 1/2, (g,h) 1/3.

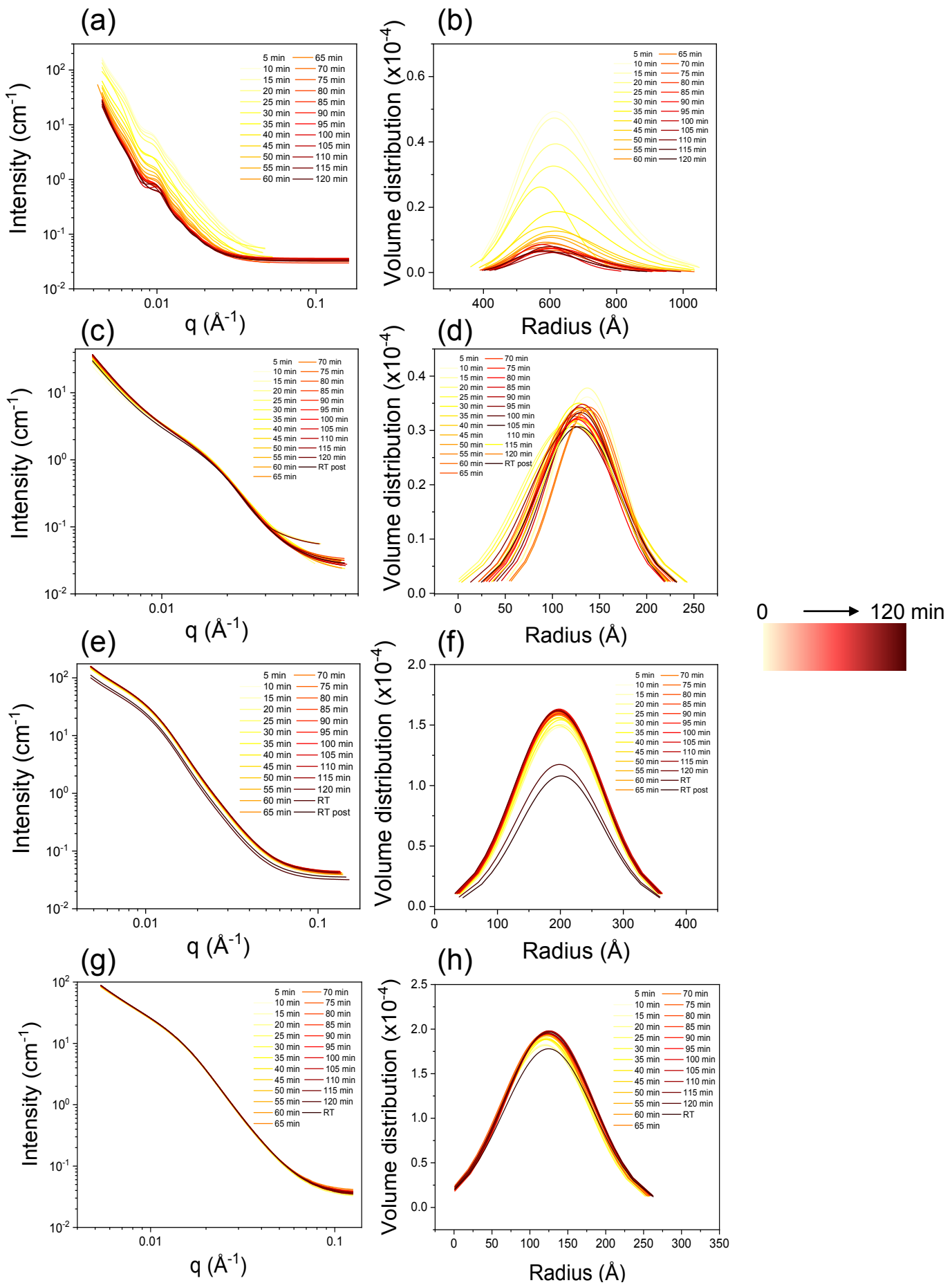


**Fig. S6.** Modelled SAXS profiles (left) and particle volume distributions (right) in different reaction times of the *in situ* conversion of hydroxycarbonates into vanadate particles  $[(\text{Y}_{0.95}\text{Eu}_{0.05})\text{VO}_4]$  in different  $\text{H}_2\text{O}/\text{EG}$  ratios: (a,b) 3/2, (c,d) 1/1, (e,f) 1/2, (g,h) 1/3.

**Table S2.** Data calculated from SAXS fittings to estimate the concentration of particles in suspension at different times during the formation of  $(Y_{0.95}Eu_{0.05})CO_3OH.xH_2O$  particles and the conversion of hydroxycarbonate templates into final vanadates  $[(Y_{0.95}Eu_{0.05})VO_4]$  at different H<sub>2</sub>O/EG volume ratios: extrapolated intensities when  $q \rightarrow 0$  ( $I_{q=0}$ )<sup>a</sup> and associated errors ( $\pm Er$ ), particle radii, and number of particles per cubic centimetre ( $N_p$ ). The difference in scattering length densities ( $\Delta\rho$ )<sup>b</sup> is specified for each sample at the top of the columns.

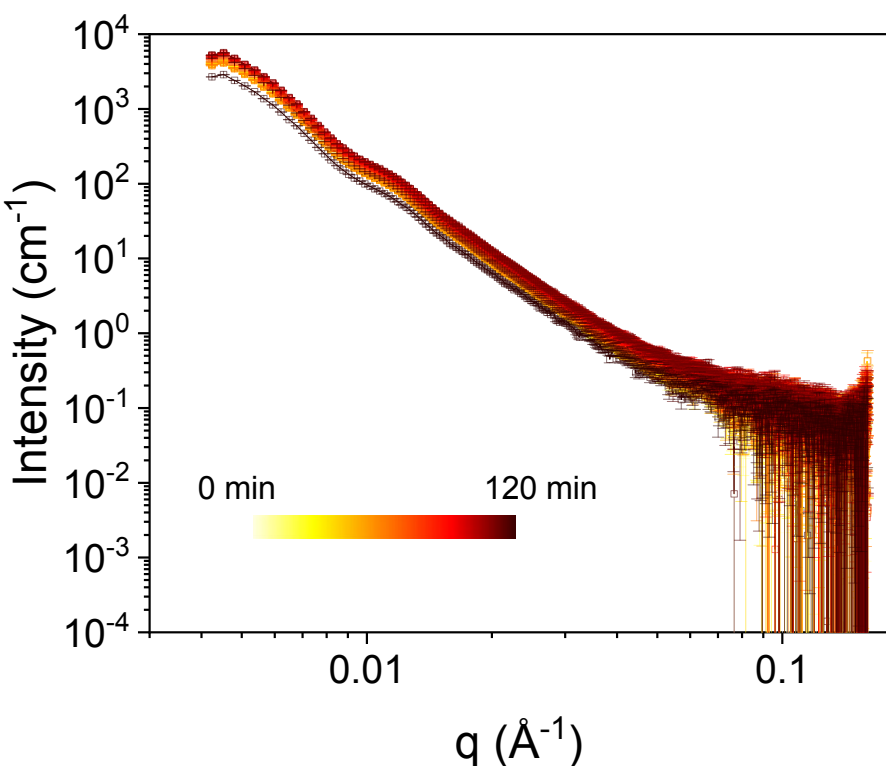
Time (min)	Hydroxycarbonate templates $[(Y_{0.95}Eu_{0.05})CO_3OH.xH_2O]$															
	H <sub>2</sub> O/EG = 3/2 ( $\Delta\rho=1.33 \times 10^{11} \text{ cm}^{-2}$ )				H <sub>2</sub> O/EG = 1/1 ( $\Delta\rho=1.32 \times 10^{11} \text{ cm}^{-2}$ )				H <sub>2</sub> O/EG = 1/2 ( $\Delta\rho=1.31 \times 10^{11} \text{ cm}^{-2}$ )				H <sub>2</sub> O/EG = 1/3 ( $\Delta\rho=1.31 \times 10^{11} \text{ cm}^{-2}$ )			
	$I_{q=0}$ ( $\text{cm}^{-1}$ )	$\pm Er$	Radius (Å)	$N_p$ ( $\text{cm}^{-3}$ )	$I_{q=0}$ ( $\text{cm}^{-1}$ )	$\pm Er$	Radius (Å)	$N_p$ ( $\text{cm}^{-3}$ )	$I_{q=0}$ ( $\text{cm}^{-1}$ )	$\pm Er$	Radius (Å)	$N_p$ ( $\text{cm}^{-3}$ )	$I_{q=0}$ ( $\text{cm}^{-1}$ )	$\pm Er$	Radius (Å)	$N_p$ ( $\text{cm}^{-3}$ )
5	0.96	1.06	--	--	--	-	-	-	0.84	1.39	-	-	8257	13830	-	-
10	4.47	119	--	--	20.79	0.93	-	-	64.0	6E+5	-	-	9.03	4E+5	-	-
15	0.27	0.34	--	--	35.12	0.84	-	-	2.22	2.59	-	-	4356	3922	-	-
20	0.52	0.29	446	$2.1 \times 10^8$	45.78	1.10	-	-	0.94	0.29	-	-	23619	36359	-	-
25	0.39	0.27	484	$9.7 \times 10^7$	63.15	1.00	-	-	1.52	0.29	85	$1.4 \times 10^{13}$	229	332	-	-
30	0.35	0.26	517	$5.8 \times 10^7$	76.34	1.17	134	$4.2 \times 10^{13}$	2.40	0.29	93	$1.2 \times 10^{13}$	6921	3359	-	-
35	2.09	4.26	--	--	94.97	2.34	139	$4.4 \times 10^{13}$	4.14	0.28	104	$1.1 \times 10^{13}$	11248	7331	-	-
40	0.72	0.26	569	$6.8 \times 10^7$	101.91	2.42	141	$4.3 \times 10^{13}$	6.61	0.36	109	$1.3 \times 10^{13}$	2114	1720	--	--
45	0.82	0.28	572	$7.5 \times 10^7$	116.72	2.42	142	$4.6 \times 10^{13}$	10.67	0.65	116	$1.4 \times 10^{13}$	1.39	0.51	30	$5.8 \times 10^{15}$
50	0.86	0.28	596	$6.1 \times 10^7$	114.60	1.05	143	$4.4 \times 10^{13}$	12.81	0.29	117	$1.6 \times 10^{13}$	0.89	0.30	42	$5.1 \times 10^{14}$
55	1.22	0.25	602	$8.2 \times 10^7$	121.06	1.41	143	$4.5 \times 10^{13}$	15.38	0.33	120	$1.7 \times 10^{13}$	1.43	0.27	38	$1.5 \times 10^{15}$
60	1.32	0.27	621	$7.4 \times 10^7$	121.26	1.10	144	$4.5 \times 10^{13}$	18.58	0.53	118	$2.3 \times 10^{13}$	1.97	0.48	41	$1.4 \times 10^{15}$
65	1.36	0.24	651	$5.7 \times 10^7$	122.64	1.58	142	$4.8 \times 10^{13}$	23.47	0.83	114	$3.5 \times 10^{13}$	1.32	0.24	47	$4.3 \times 10^{14}$
70	2.49	0.29	650	$1.1 \times 10^8$	113.17	2.25	140	$4.9 \times 10^{13}$	20.61	0.85	115	$3.0 \times 10^{13}$	2.75	1.23	42	$1.8 \times 10^{15}$
75	2.32	0.25	625	$1.2 \times 10^8$	107.65	1.23	139	$4.9 \times 10^{13}$	23.38	1.33	116	$3.3 \times 10^{13}$	3.50	1.68	43	$1.9 \times 10^{15}$
80	2.15	0.22	638	$1.0 \times 10^8$	95.10	1.18	135	$5.1 \times 10^{13}$	25.88	0.59	115	$3.7 \times 10^{13}$	3.90	1.31	47	$1.2 \times 10^{15}$
85	2.38	0.32	629	$1.2 \times 10^8$	85.20	1.07	132	$5.3 \times 10^{13}$	21.39	0.70	113	$3.4 \times 10^{13}$	2.83	0.84	45	$1.1 \times 10^{15}$
90	2.69	0.27	633	$1.4 \times 10^8$	85.14	0.96	130	$5.7 \times 10^{13}$	23.71	0.79	114	$3.5 \times 10^{13}$	2.64	0.29	47	$8.7 \times 10^{14}$
95	2.91	0.28	610	$1.8 \times 10^8$	87.93	1.44	130	$6.0 \times 10^{13}$	22.94	0.45	112	$3.8 \times 10^{13}$	2.86	0.29	46	$9.6 \times 10^{14}$
100	3.06	0.29	620	$1.7 \times 10^8$	91.62	1.31	130	$6.1 \times 10^{13}$	28.48	0.61	112	$4.8 \times 10^{13}$	2.93	0.29	45	$1.2 \times 10^{15}$
105	2.88	0.27	620	$1.6 \times 10^8$	87.95	1.24	129	$6.2 \times 10^{13}$	30.26	0.74	113	$4.7 \times 10^{13}$	2.83	0.31	47	$8.8 \times 10^{14}$
110	2.61	0.25	624	$1.4 \times 10^8$	86.45	1.23	129	$6.0 \times 10^{13}$	22.66	0.49	113	$3.6 \times 10^{13}$	3.67	0.41	43	$1.8 \times 10^{15}$
115	2.67	0.30	634	$1.3 \times 10^8$	85.95	1.29	128	$6.3 \times 10^{13}$	18.19	0.37	112	$3.1 \times 10^{13}$	3.17	0.35	46	$1.1 \times 10^{15}$
120	2.84	0.27	619	$1.6 \times 10^8$	85.04	1.20	128	$6.2 \times 10^{13}$	18.41	0.55	109	$3.6 \times 10^{13}$	3.30	0.35	43	$1.6 \times 10^{15}$

Table S2 (cont.).

Vanadate Nanoparticles $[(Y_{0.95}Eu_{0.05})VO_4]$																
Time (min)	H <sub>2</sub> O/EG = 3/2 ( $\Delta\rho=2.43\times10^{11}$ cm <sup>-2</sup> )				H <sub>2</sub> O/EG = 1/1 ( $\Delta\rho=2.42\times10^{11}$ cm <sup>-2</sup> )				H <sub>2</sub> O/EG = 1/2 ( $\Delta\rho=2.39\times10^{11}$ cm <sup>-2</sup> )				H <sub>2</sub> O/EG = 1/3 ( $\Delta\rho=2.32\times10^{11}$ cm <sup>-2</sup> )			
	I <sub>q=0</sub> (cm <sup>-1</sup> )	±Er	Radius (Å)	N <sub>P</sub> (cm <sup>-3</sup> )	I <sub>q=0</sub> (cm <sup>-1</sup> )	±Er	Radius (Å)	N <sub>P</sub> (cm <sup>-3</sup> )	I <sub>q=0</sub> (cm <sup>-1</sup> )	±Er	Radius (Å)	N <sub>P</sub> (cm <sup>-3</sup> )	I <sub>q=0</sub> (cm <sup>-1</sup> )	±Er	Radius (Å)	N <sub>P</sub> (cm <sup>-3</sup> )
5	25.95	2.23	655	3.2E+08	2.56	0.52	118	9.4E+11	5.65	0.26	199	9.0E+10	34.35	1.29	117	1.4E+13
10	1.00	0.24	654	1.2E+07	8.00	0.56	126	1.9E+12	5.70	0.49	199	9.2E+10	37.99	1.35	123	1.2E+13
15	5.63	0.58	650	7.2E+07	8.33	0.59	127	1.9E+12	6.53	0.50	200	1.0E+11	37.46	1.06	121	1.3E+13
20	4.04	0.42	657	4.9E+07	7.39	0.62	124	2.0E+12	3.10	0.37	200	4.8E+10	37.17	1.09	122	1.2E+13
25	3.71	0.46	650	4.8E+07	3.61	0.48	121	1.1E+12	4.10	0.43	197	7.0E+10	37.42	1.31	122	1.2E+13
30	1.48	0.37	660	1.7E+07	14.43	1.27	128	3.2E+12	4.75	0.77	197	8.0E+10	36.42	1.21	121	1.2E+13
35	1.65	0.37	659	1.9E+07	5.86	0.66	123	1.6E+12	5.86	0.66	201	9.0E+10	40.89	1.16	124	1.2E+13
40	1.44	0.36	629	2.2E+07	3.86	0.32	128	8.5E+11	4.53	0.33	197	7.7E+10	30.63	0.76	122	9.7E+12
45	0.94	0.34	653	1.2E+07	4.22	0.44	128	9.1E+11	4.75	0.37	198	7.9E+10	40.82	0.89	123	1.3E+13
50	1.27	0.37	640	1.8E+07	6.10	0.60	127	1.4E+12	5.92	0.67	198	9.7E+10	41.61	1.07	124	1.2E+13
55	0.54	0.20	629	8.4E+06	3.60	0.82	131	7.0E+11	4.81	0.42	197	8.1E+10	40.90	1.12	123	1.2E+13
60	0.55	0.33	619	9.4E+06	3.31	0.33	126	7.9E+11	3.04	0.32	197	5.2E+10	41.92	0.98	122	1.3E+13
65	0.34	0.28	627	5.4E+06	7.68	0.60	124	2.1E+12	4.43	0.49	197	7.5E+10	32.24	1.11	124	9.6E+12
70	1.17	0.30	647	1.5E+07	6.21	1.37	126	1.5E+12	4.95	0.60	198	8.2E+10	26.23	1.11	123	8.0E+12
75	0.48	0.25	607	9.3E+06	3.84	0.35	128	8.4E+11	4.25	0.43	197	7.2E+10	38.30	0.84	123	1.2E+13
80	0.60	0.31	630	9.3E+06	4.18	0.38	129	8.8E+11	4.32	0.37	197	7.4E+10	40.37	0.76	125	1.1E+13
85	0.83	0.23	632	1.3E+07	4.06	0.34	132	7.5E+11	4.10	0.36	197	7.0E+10	25.68	0.79	126	7.0E+12
90	0.93	0.33	642	1.3E+07	4.32	0.30	129	9.1E+11	4.22	0.43	196	7.3E+10	25.68	0.86	126	6.8E+12
95	1.89	0.38	643	2.6E+07	4.53	0.41	122	1.3E+12	4.67	0.40	198	7.7E+10	23.84	1.01	125	6.7E+12
100	2.29	0.49	592	5.1E+07	3.78	0.29	130	7.5E+11	4.12	0.41	198	6.8E+10	25.85	1.09	125	7.2E+12
105	1.27	4.51	607	2.4E+07	3.79	0.34	128	8.3E+11	1.76	0.31	198	2.9E+10	29.00	1.26	127	7.5E+12
110	1.26	0.46	654	1.5E+07	3.62	0.36	129	7.6E+11	1.96	0.38	196	3.4E+10	34.83	1.29	126	9.4E+12
115	1.19	0.71	620	2.0E+07	3.38	0.36	129	7.1E+11	3.55	0.53	196	6.2E+10	36.49	2.35	125	1.0E+13
120	0.89	0.25	607	1.7E+07	4.10	0.52	128	9.3E+11	3.83	0.42	196	6.7E+10	48.69	0.97	126	1.3E+13

<sup>a</sup> Extrapolated intensities when q→0 (I<sub>q=0</sub>) were estimated using by Guinier fits of experimental data using the SASfit 0.93.4 package.<sup>5</sup>

<sup>b</sup> Scattering length densities (SLD) of solvent mixtures were calculated considering experimental molar fractions and tabulated volumetric mass densities.<sup>6</sup> SLD of particles were calculated assuming a volumetric mass density of 2.8 g cm<sup>-3</sup> for hydroxycarbonates, and using volumetric mass densities estimated from XRD results for vanadate nanoparticles, namely 4.310, 4.308, 4.278, and 4.194 g cm<sup>-3</sup> for particles prepared in H<sub>2</sub>O/EG volume ratios of 3/2, 1/1, 1/2 and 1/3, respectively.



**Fig. S7.** Time dependent SAXS profiles of the two-step conversion of hydroxycarbonate particles (prepared in H<sub>2</sub>O/EG=3/2) into (Y<sub>0.95</sub>Eu<sub>0.05</sub>)VO<sub>4</sub> nanoparticles in water.

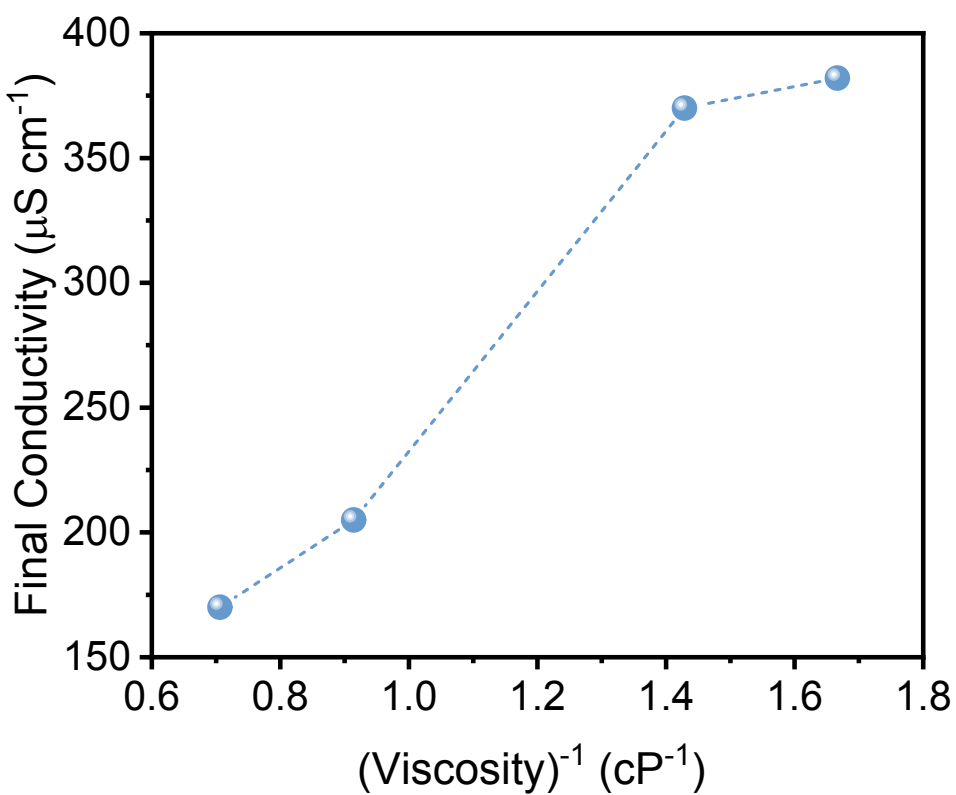


**Fig. S8.** Variation of experimental conductivities ( $\kappa$ ) of urea solutions (1.25 mol L<sup>-1</sup>) in different H<sub>2</sub>O/EG mixtures (namely 3/2, 1/1, 1/2, and 1/3, vol./vol.) at 95 °C with the viscosity ( $\eta$ ) of the solvent mixture,<sup>6</sup> highlighting the non-linear dependence of  $\kappa$  against  $1/\eta$ .

## 2.4. Additional Microscopy Images

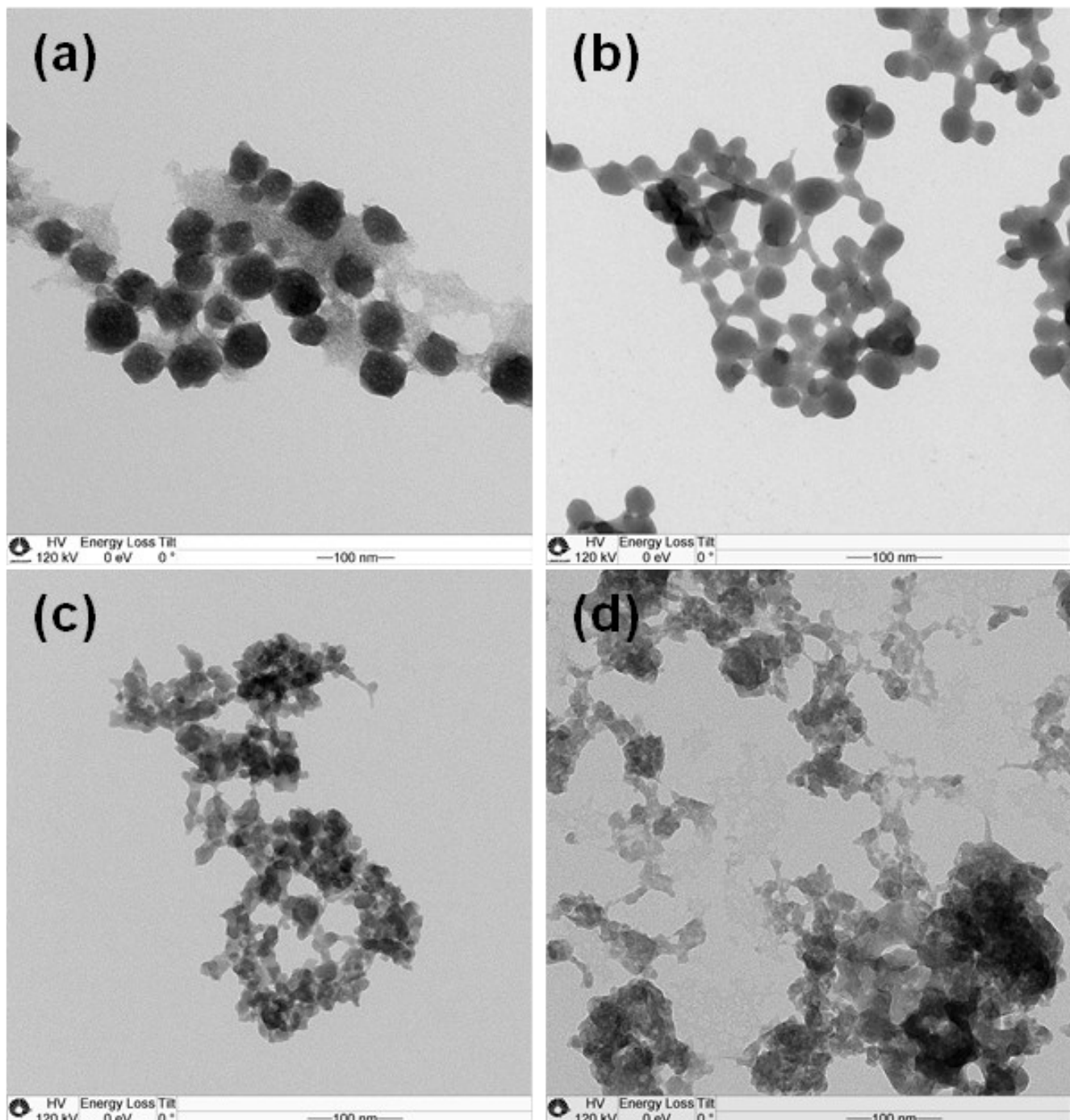


**Fig. S9.** TEM images of  $(Y_{0.95}Eu_{0.05})CO_3OH \cdot xH_2O$  particles prepared in different  $H_2O/EG$  (vol./vol.) mixtures: (a) 3/2, (b) 1/1, (c) 1/2, (d) 1/3.

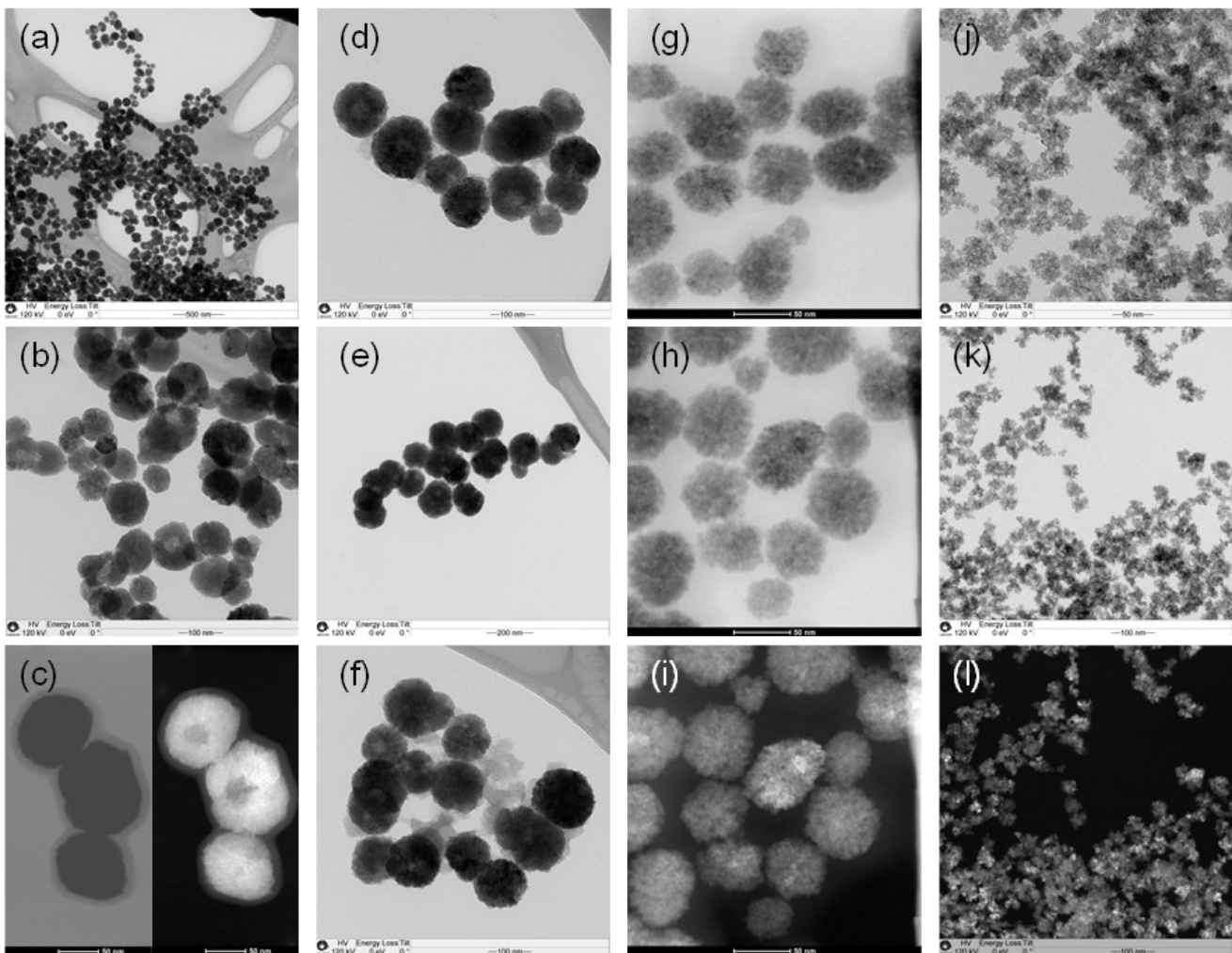


**Fig S10.** TEM images of (Y<sub>0.95</sub>Eu<sub>0.05</sub>)VO<sub>4</sub> particles prepared by one-pot conversion of hydroxycarbonates in different H<sub>2</sub>O/EG (vol./vol.) mixtures: (a-c) 3/2, (d-f) 1/1, (g-i) 1/2, (j-l) 1/3.

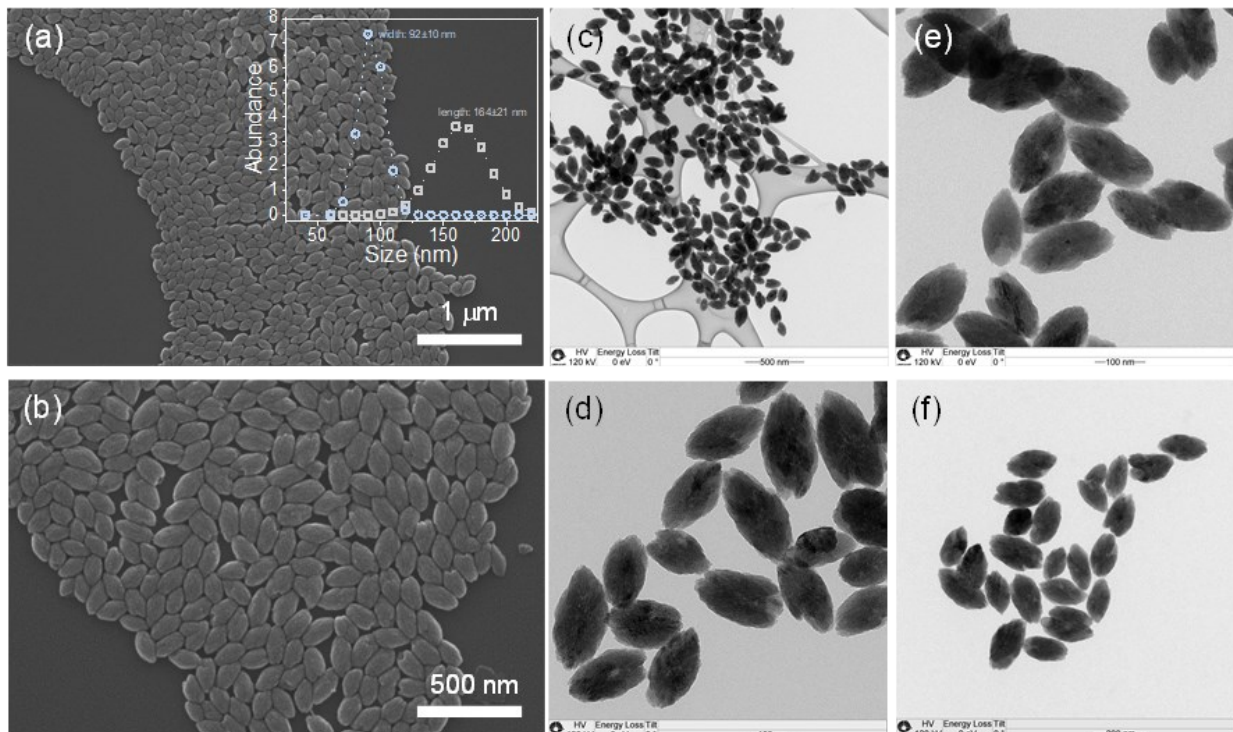


**Fig S11.** (a-b) SEM and (c-f) TEM images of the (Y<sub>0.95</sub>Eu<sub>0.05</sub>)VO<sub>4</sub> particles prepared via two-step conversion of hydroxycarbonate templates in water. Inset in (a) shows size distributions obtained from TEM images.

## 2.5. FTIR spectra of (Y,Eu)VO<sub>4</sub> nanoparticles

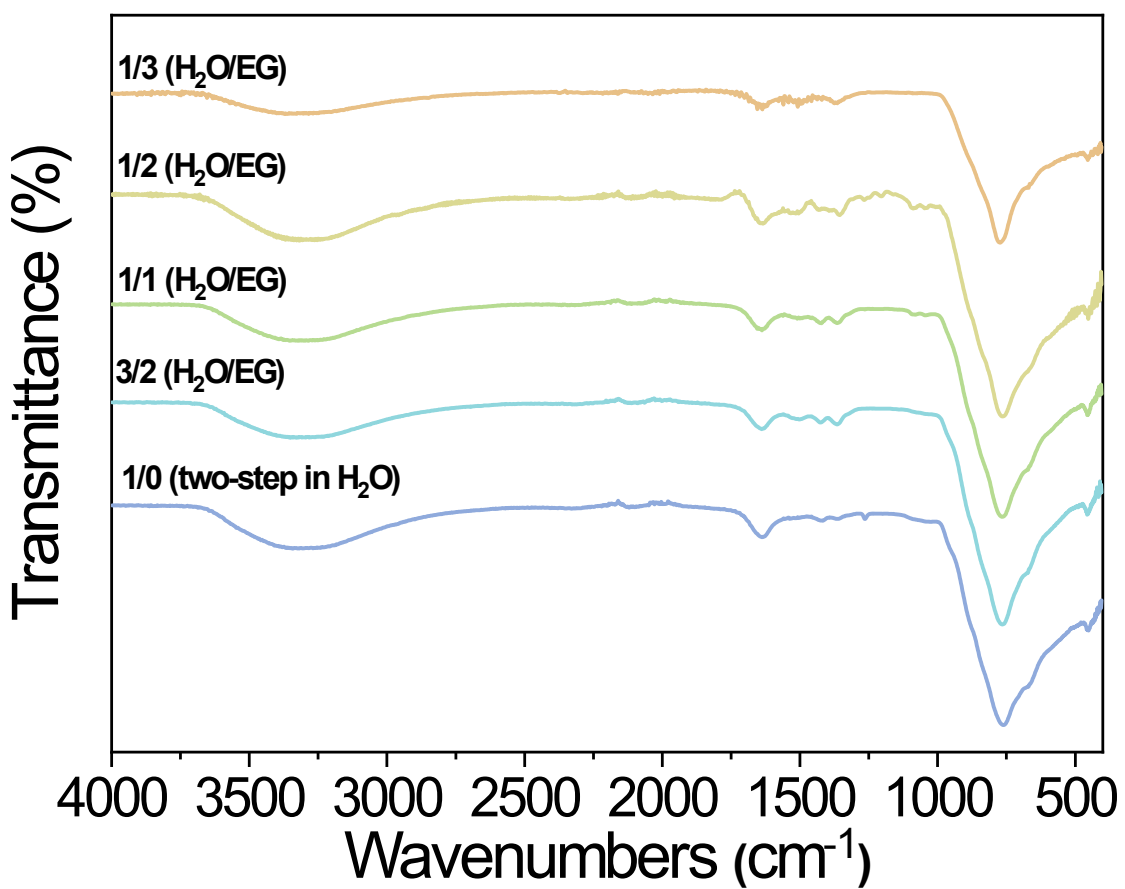


**Fig. S12.** Infrared spectra of the vanadate nanoparticles [ $(Y_{0.95}Eu_{0.05})VO_4$ ] prepared via colloidal one-pot conversion of RE hydroxycarbonates in different  $H_2O/EG$  volume ratios from 1/3 (top) to 3/2 and by two-step conversion in pure water (bottom).

## 2.6. N<sub>2</sub> Adsorption Isotherms

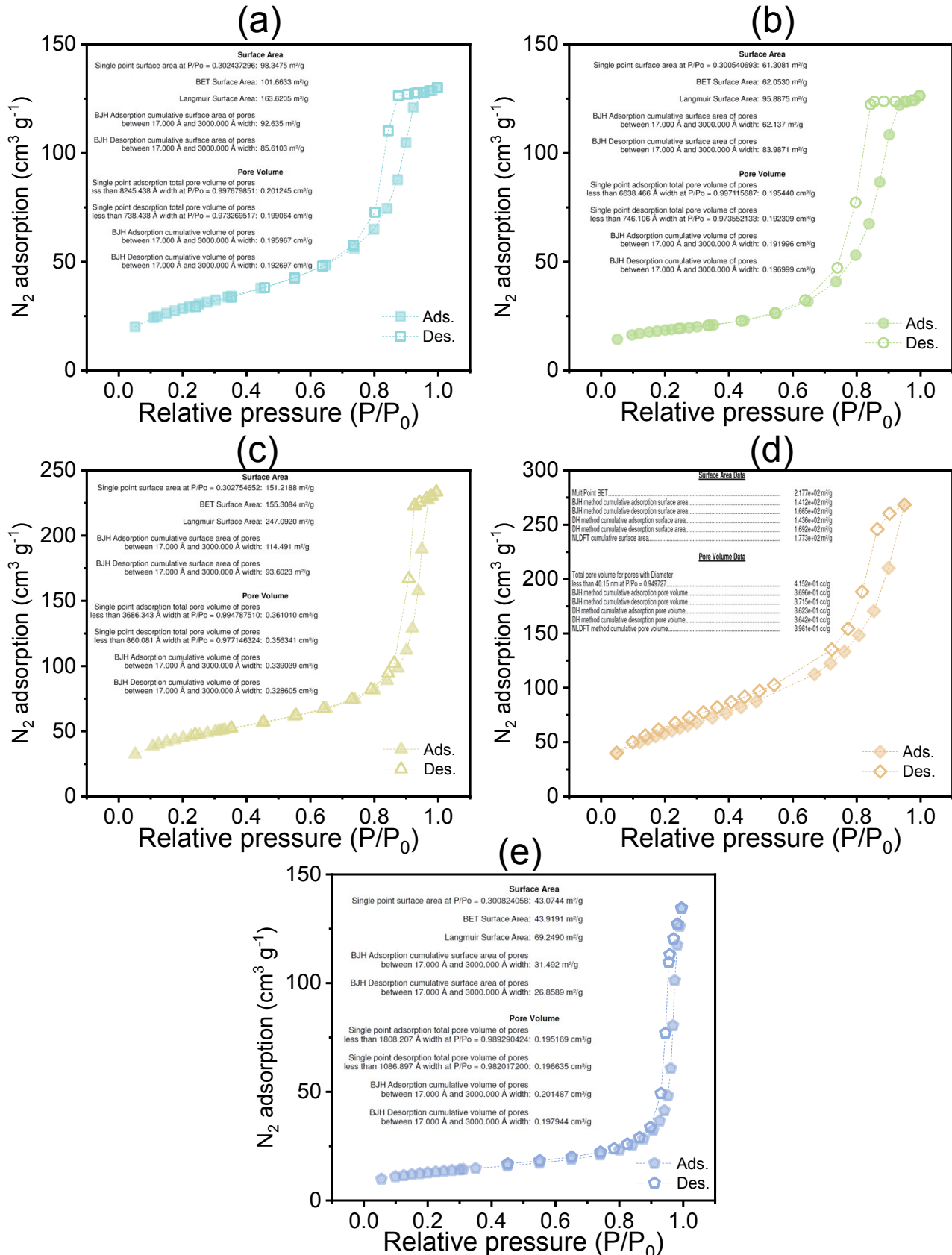


**Fig. S13.** N<sub>2</sub> adsorption/desorption isotherms of the (Y<sub>0.95</sub>Eu<sub>0.05</sub>)VO<sub>4</sub> nanoparticles prepared by colloidal conversion of hydroxycarbonates in different H<sub>2</sub>O/EG volume ratios: (a) 3/2, (b) 1/1, (c) 1/2, (d) 1/3, (e) 1/0 (pure water, two-step conversion). Insets show surface area and porosity results of BET and BJH treatments on experimental data.

## 2.7. XRD data

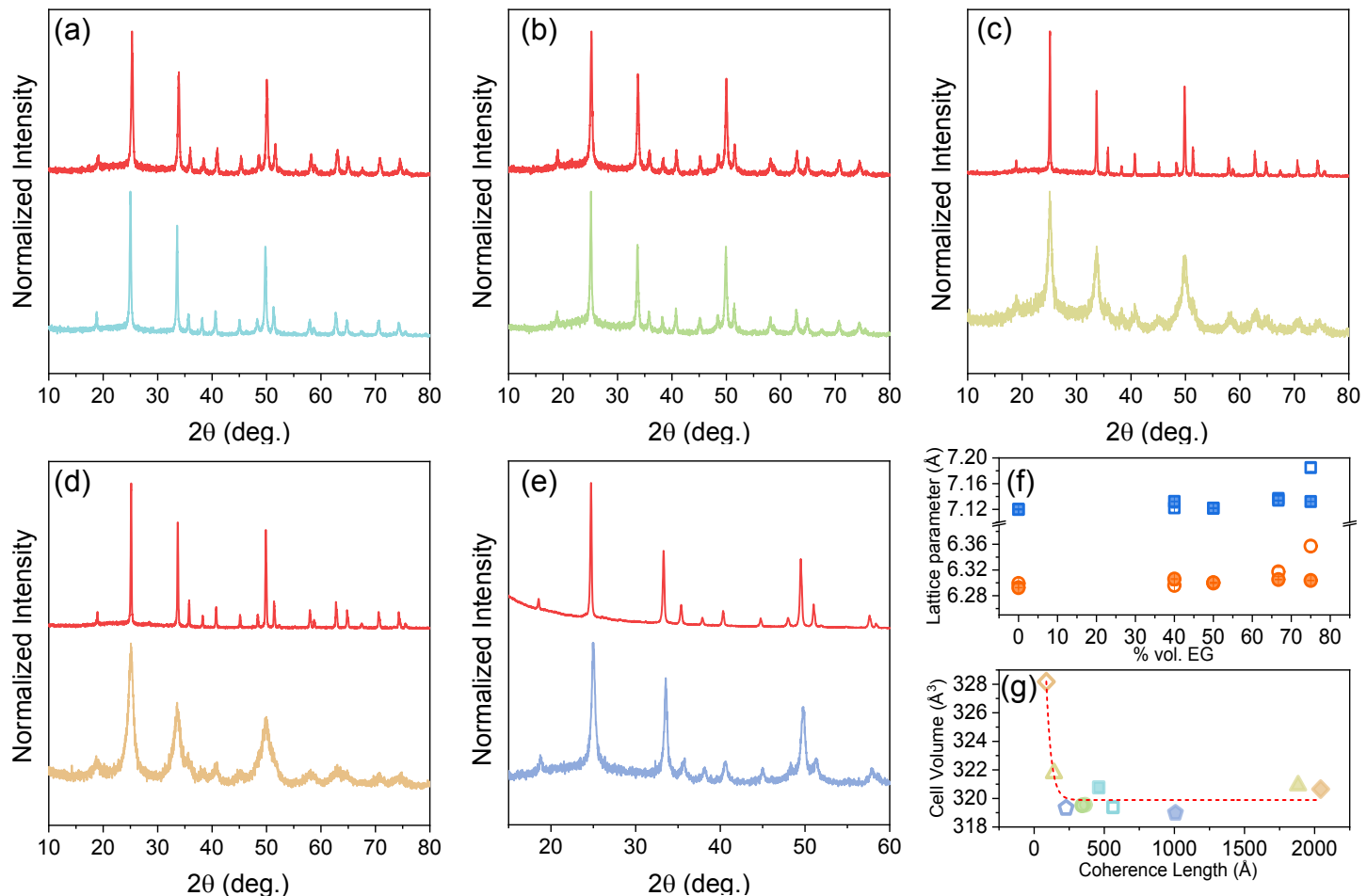


**Fig S14.** (a-e) XRD profiles of  $(\text{Y}_{0.95}\text{Eu}_{0.05})\text{VO}_4$  samples prepared by conversion of hydroxycarbonates in different H<sub>2</sub>O/EG volume ratios before (bottom curves, as prepared samples) and after (top red curves) calcination at 900 °C for 30 min, H<sub>2</sub>O/EG= (a) 3/2, (b) 1/1, (c) 1/2, (d) 1/3, and (e) 1/0 (two-step conversion, pure water). (f) Variation of cell parameters *a* (blue) and *c* (orange) of the *I4<sub>1</sub>/amd* tetragonal structure of the  $(\text{Y}_{0.95}\text{Eu}_{0.05})\text{VO}_4$  powders with the amount (% vol.) of EG used in the synthesis and (g) dependence of cell volumes on the crystalline coherence length for as prepared (empty symbols) and calcined (filled symbols) samples.

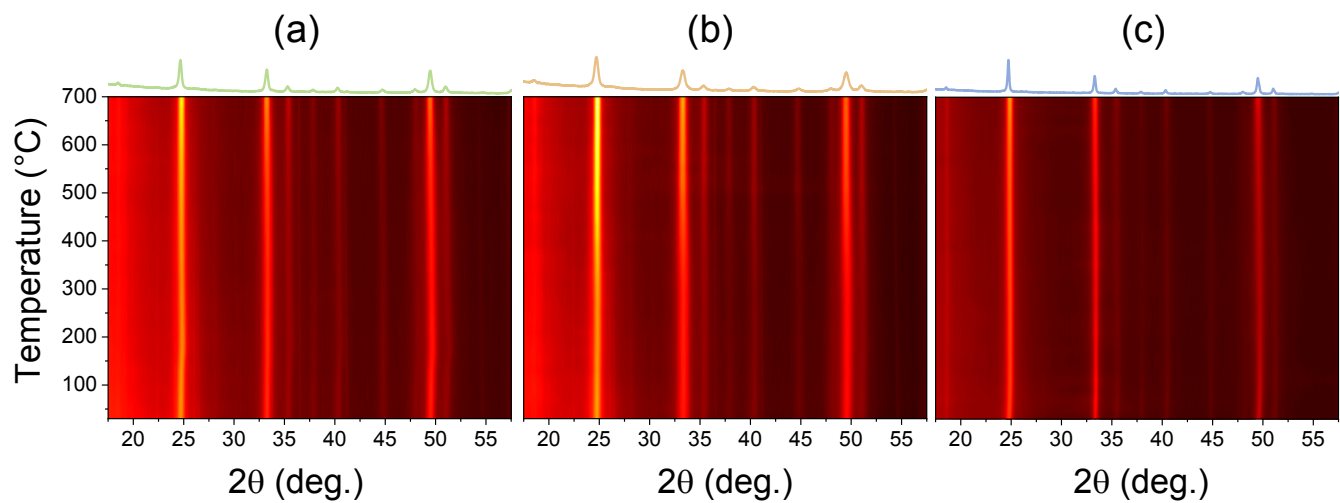


**Fig S15.** Representative thermodiffraction profiles of  $(Y_{0.95}Eu_{0.05})VO_4$  powder samples prepared in  $H_2O/EG =$  (a) 1/1, (b) 1/3 and (c) 1/0 (two step conversion in pure water). Diffraction profiles at the top correspond were acquired after the heating ramps with samples cooled to room temperature.

## 2.8. Thermogravimetry of (Y,Eu)VO<sub>4</sub> nanoparticles

**Table S3.** Results calculated from TGA analysis of (Y<sub>0.95</sub>Eu<sub>0.05</sub>)VO<sub>4</sub> nanoparticles (Fig. 5(a)): initial mass ( $m_0$ ), mass percentages after the first and second decomposition steps, residues at 600 °C ( $m_f$ ), and mass increase (relative to  $m_f$ ) at 900 °C

H <sub>2</sub> O/EG (vol/vol) =	$m_0$ (mg)	Mass		Residue at 600 °C (m <sub>f</sub> ) (mg)	Mass increase at 900 °C (%m <sub>f</sub> )
		1 <sup>st</sup> step (%m <sub>0</sub> )	2 <sup>nd</sup> step (%m <sub>0</sub> )		
3/2	6.372	96.91	91.34	5.851	0.509
1/1	9.056	96.16	89.94	8.180	0.276
1/2	7.386	95.02	88.07	6.554	0.424
1/3	7.235	93.14	86.67	6.328	0.481

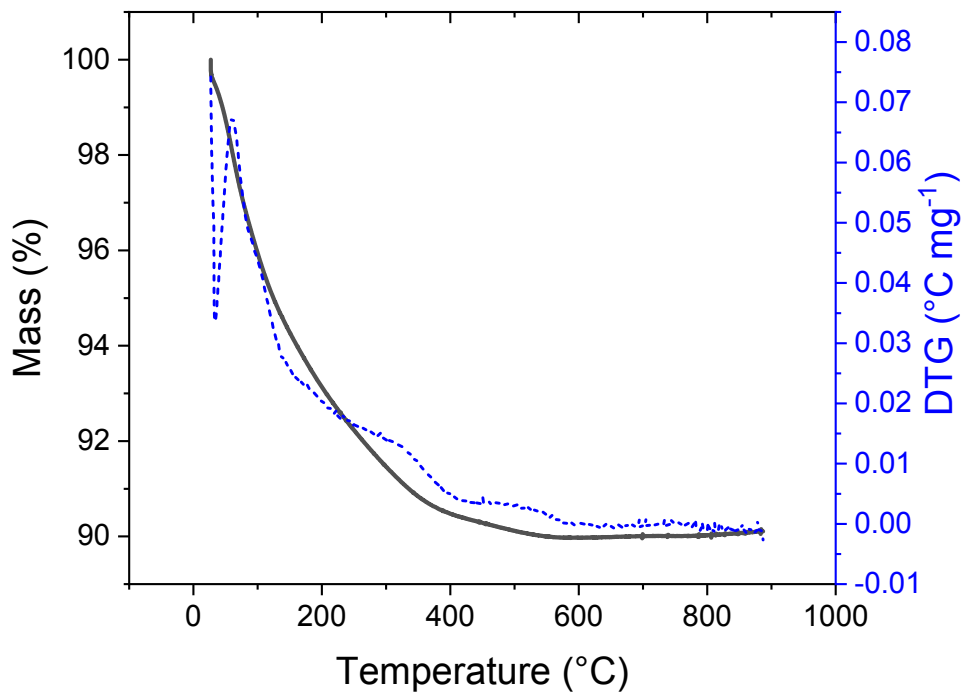


**Fig. S16.** TGA and DTG (dotted blue line) of the (Y<sub>0.95</sub>Eu<sub>0.05</sub>)VO<sub>4</sub> sample synthesized by one-pot conversion of hydroxycarbonate particles in H<sub>2</sub>O/EG=3/2 (vol./vol.) in N<sub>2</sub> atmosphere.

## 2.9. XPS Spectra

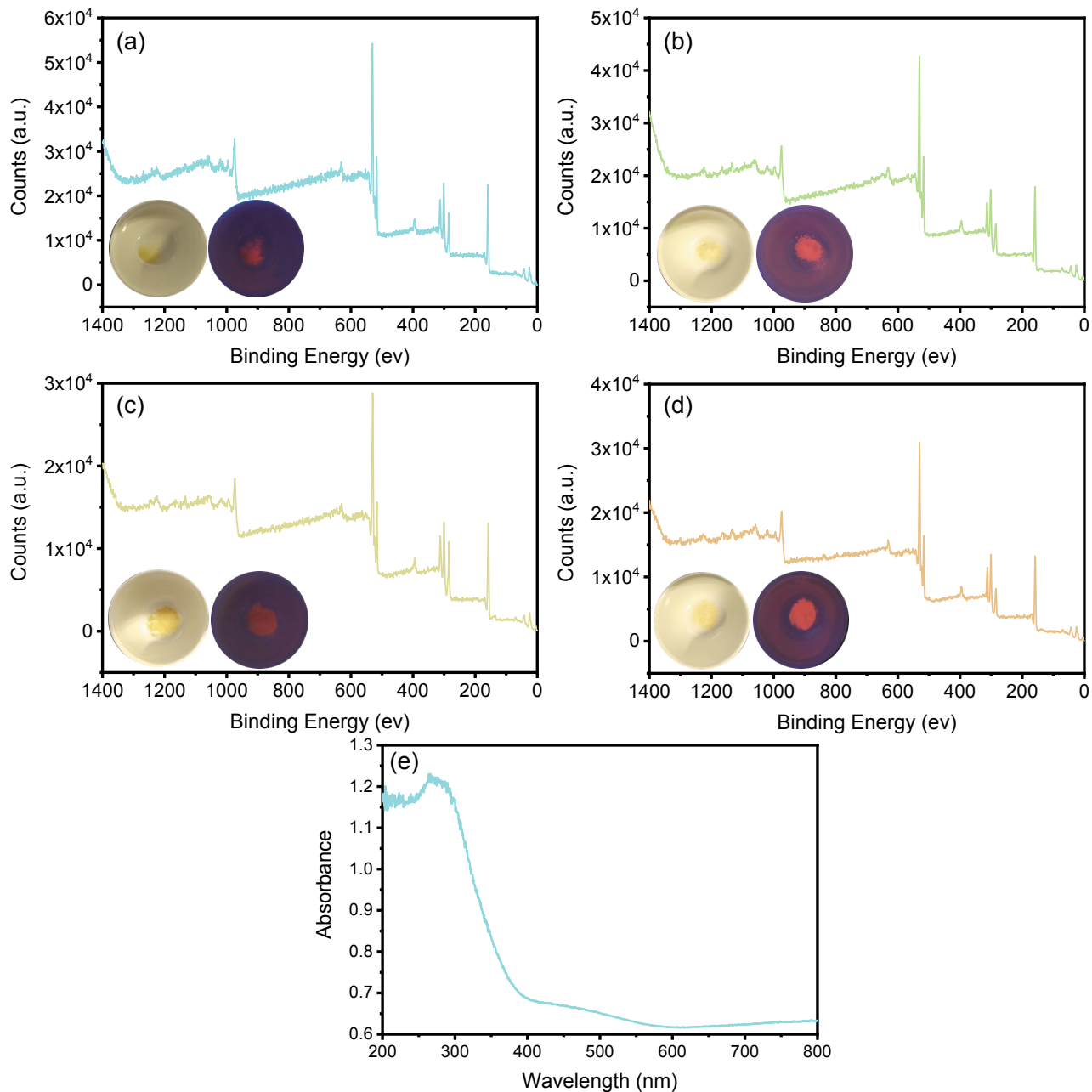


**Fig. S17.** Survey XPS spectra of  $(Y_{0.95}Eu_{0.05})VO_4$  nanoparticles prepared in different  $H_2O/EG$  volume ratios, namely (a) 3/2, (b) 1/1, (c) 1/2, (d) 1/3. (e) Representative absorption spectrum of the  $(Y_{0.95}Eu_{0.05})VO_4$  powder particles synthesized in  $H_2O/EG=3/2$ ; this spectrum was acquired via diffuse reflectance on a Agilent Cary 50 UV-Vis-NIR spectrometer using  $BaSO_4$  as blank. Insets in (a)-(d) show photographs of the respective  $(Y_{0.95}Eu_{0.05})VO_4$  solids under white light (left) and UV light (254 nm, right), highlighting the pale yellow colour of the powders and their red luminescence.

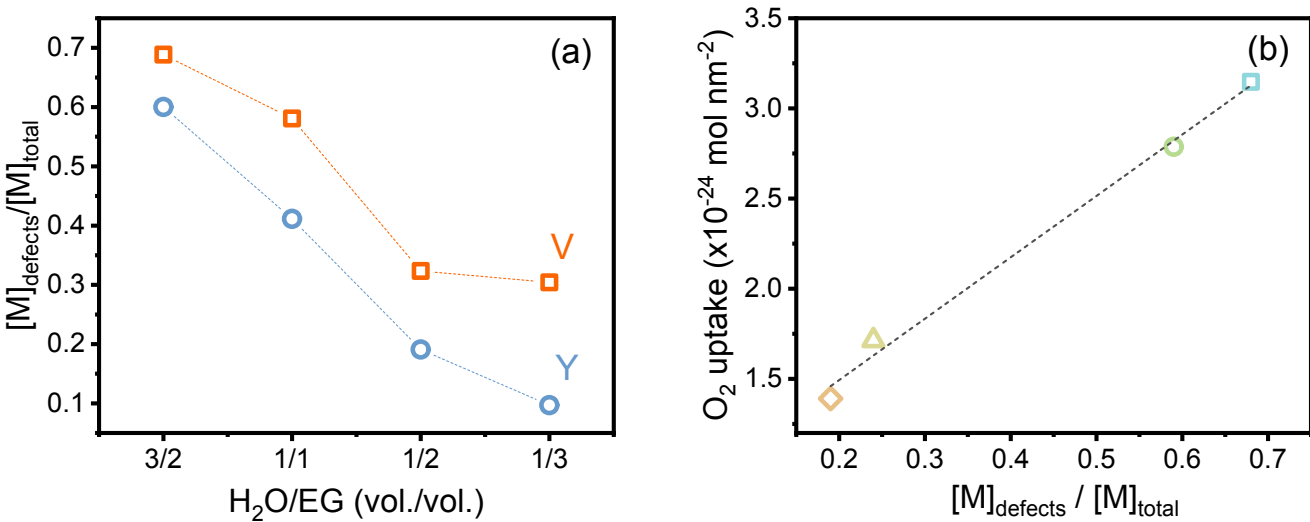


**Fig. S18.** (a) Ratios between molar percentages of partially reduced metal sites  $[M]_{\text{defects}}$  and total metal percentages  $[M]_{\text{total}}$  at the surface of  $(\text{Y}_{0.95}\text{Eu}_{0.05})\text{VO}_4$  nanoparticles obtained in different  $\text{H}_2\text{O}/\text{EG}$  volume ratios. Molar percentages were obtained from XPS spectra via deconvolution of V 2p and Y 3d signals. For vanadium (orange),  $M_{\text{defects}}$  comprise V(III) and V(IV) 2p<sub>3/2</sub> and 2p<sub>1/2</sub> signals; for yttrium (blue)  $M_{\text{defects}}$  comprise satellite peaks in 3d<sub>5/2</sub> and 3d<sub>3/2</sub> signals. (b) Correlation between  $\text{O}_2$  uptakes per area (Fig. 5) and the percentage of defect metal sites at the surface calculated from XPS analysis. In (b),  $[M]_{\text{defects}}/[M]_{\text{total}}$  comprise both yttrium and vanadium.

## 2.10. Luminescence spectra

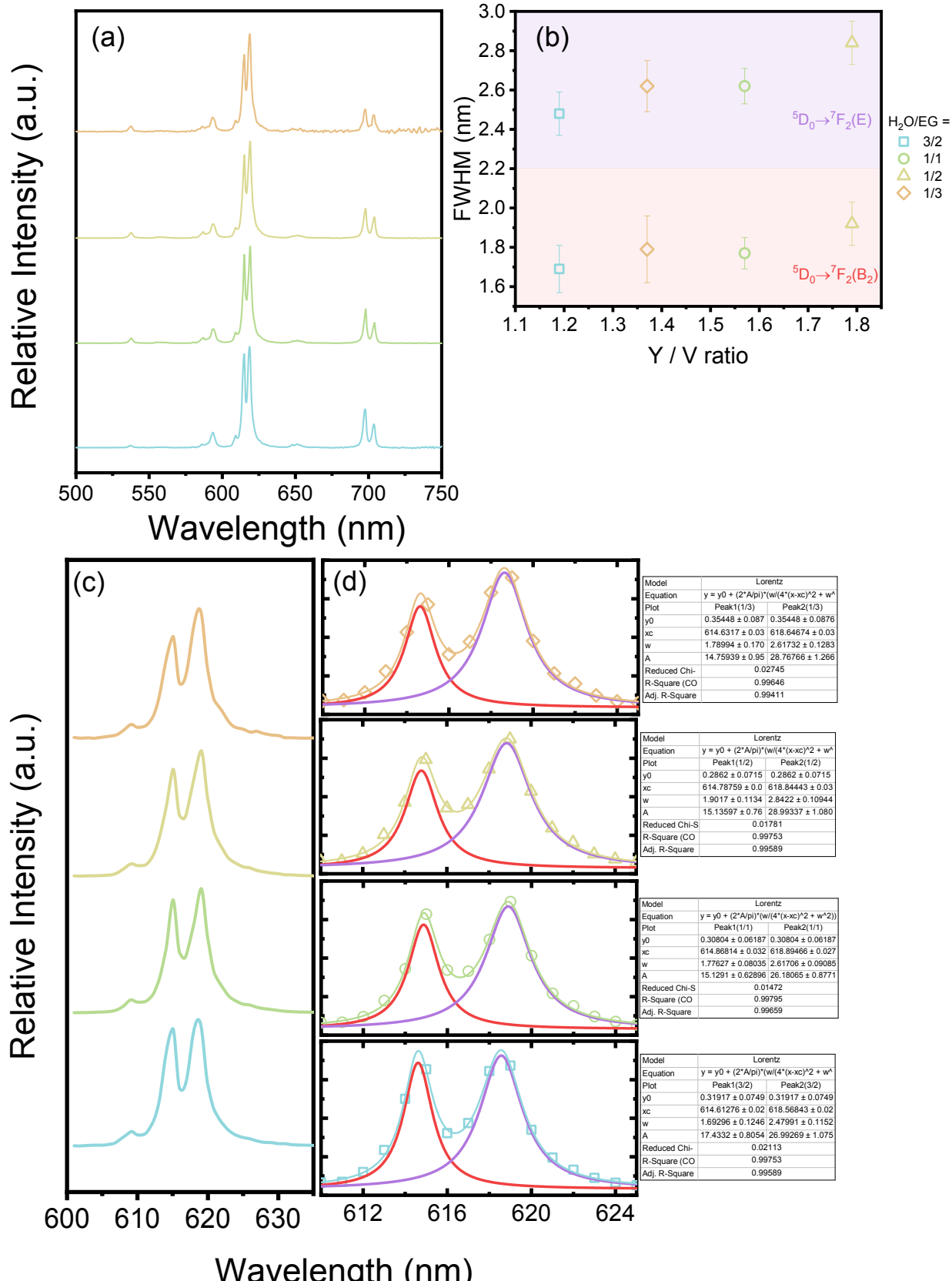


**Fig. S19.** (a) Emission spectra of (Y<sub>0.95</sub>Eu<sub>0.05</sub>)VO<sub>4</sub> nanoparticles prepared by one-pot conversion of hydroxycarbonates in different H<sub>2</sub>O/EG (vol./vol.) conditions [3/2 – blue (bottom); 1/1 – green; 1/2 – dark yellow; 1/3 – orange (top)] under UV excitation ( $\lambda_{exc}$ =280 nm). (b) Correlation between full width at half maximum (FWHM) of Lorentzian peaks of <sup>5</sup>D<sub>0</sub>→<sup>7</sup>F<sub>2</sub>(B<sub>2</sub>) and <sup>5</sup>D<sub>0</sub>→<sup>7</sup>F<sub>2</sub>(E) components with the Y/V ratio estimated from XPS for the different (Y<sub>0.95</sub>Eu<sub>0.05</sub>)VO<sub>4</sub> nanoparticles. (c) Amplification of the <sup>5</sup>D<sub>0</sub>→<sup>7</sup>F<sub>2</sub> region from emission spectra in (a). (d) Deconvolution of <sup>5</sup>D<sub>0</sub>→<sup>7</sup>F<sub>2</sub> Stark components (B<sub>2</sub>, red and E, magenta) into Lorentzian peaks.

## 2.11. Luminescence decay curves

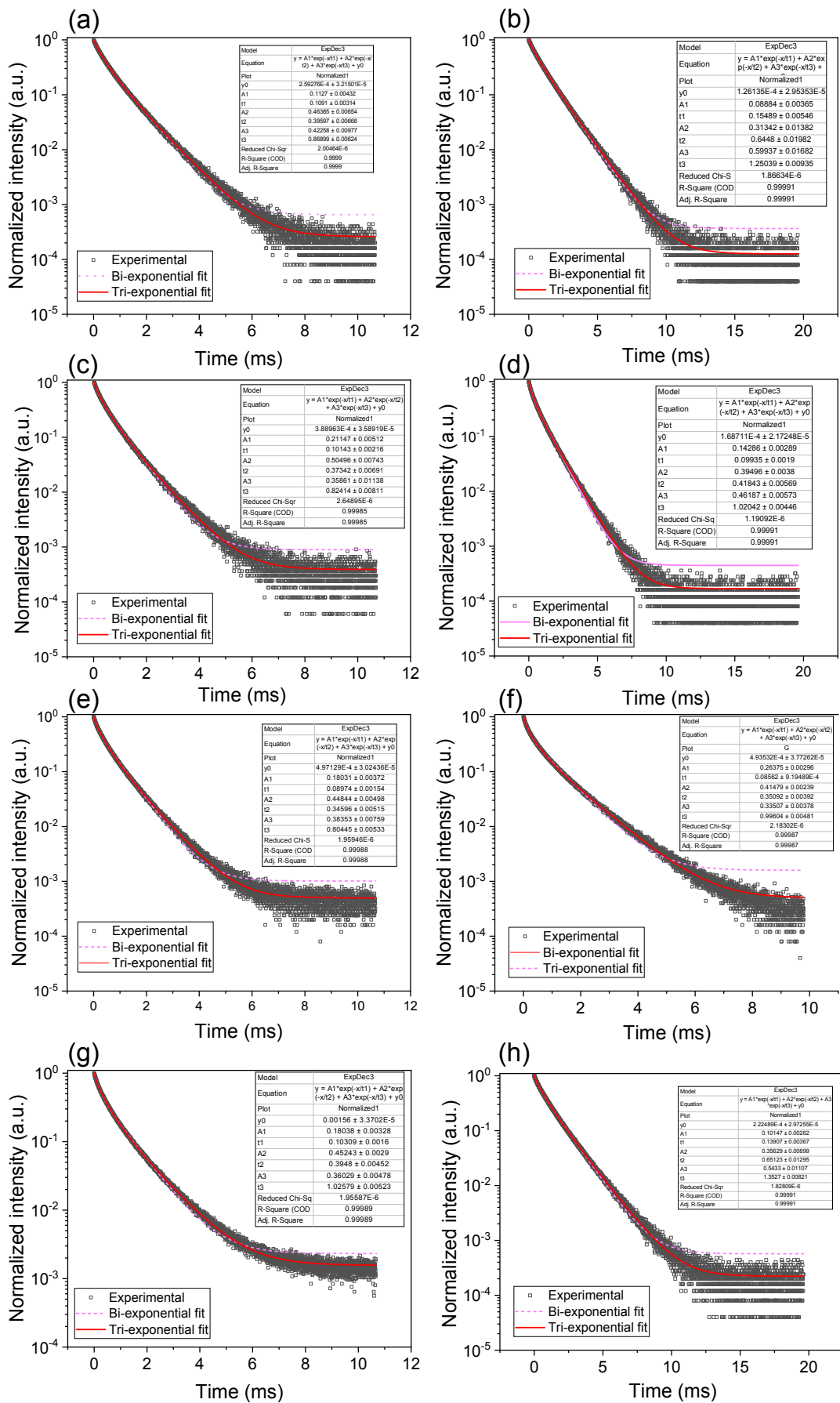


**Fig. S20.** Luminescence lifetimes ( ${}^5D_0$ ) in (a,c,e,g)  $H_2O$  or (b,d,f,h)  $D_2O$  of  $(Y_{0.95}Eu_{0.05})VO_4$  nanoparticles prepared by one-pot conversion of hydroxycarbonates in different  $H_2O/EG$  (vol/vol) solvent conditions, namely (a,b) 3/2, (c,d) 1/1, (e,f) 1/2, (g,h) 1/3.

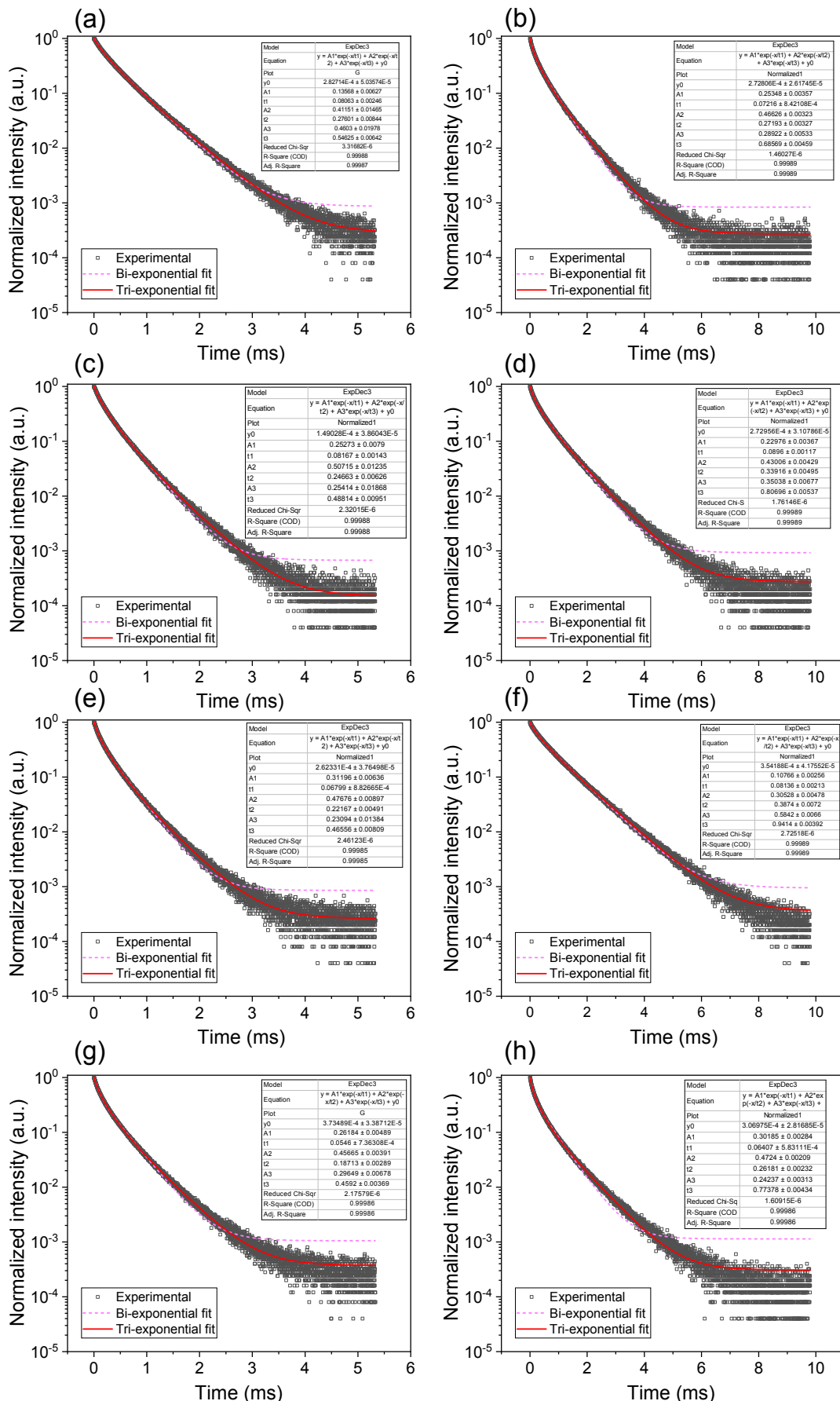


**Fig. S21.** Luminescence lifetimes ( ${}^5D_0$ ) in (a,c,e,g)  $H_2O$  or (b,d,f,h)  $D_2O$  of  $(Y_{0.80}Eu_{0.20})VO_4$  nanoparticles prepared by one-pot conversion of hydroxycarbonates in different  $H_2O/EG$  (vol/vol) solvent conditions, namely (a,b) 3/2, (c,d) 1/1, (e,f) 1/2, (g,h) 1/3.

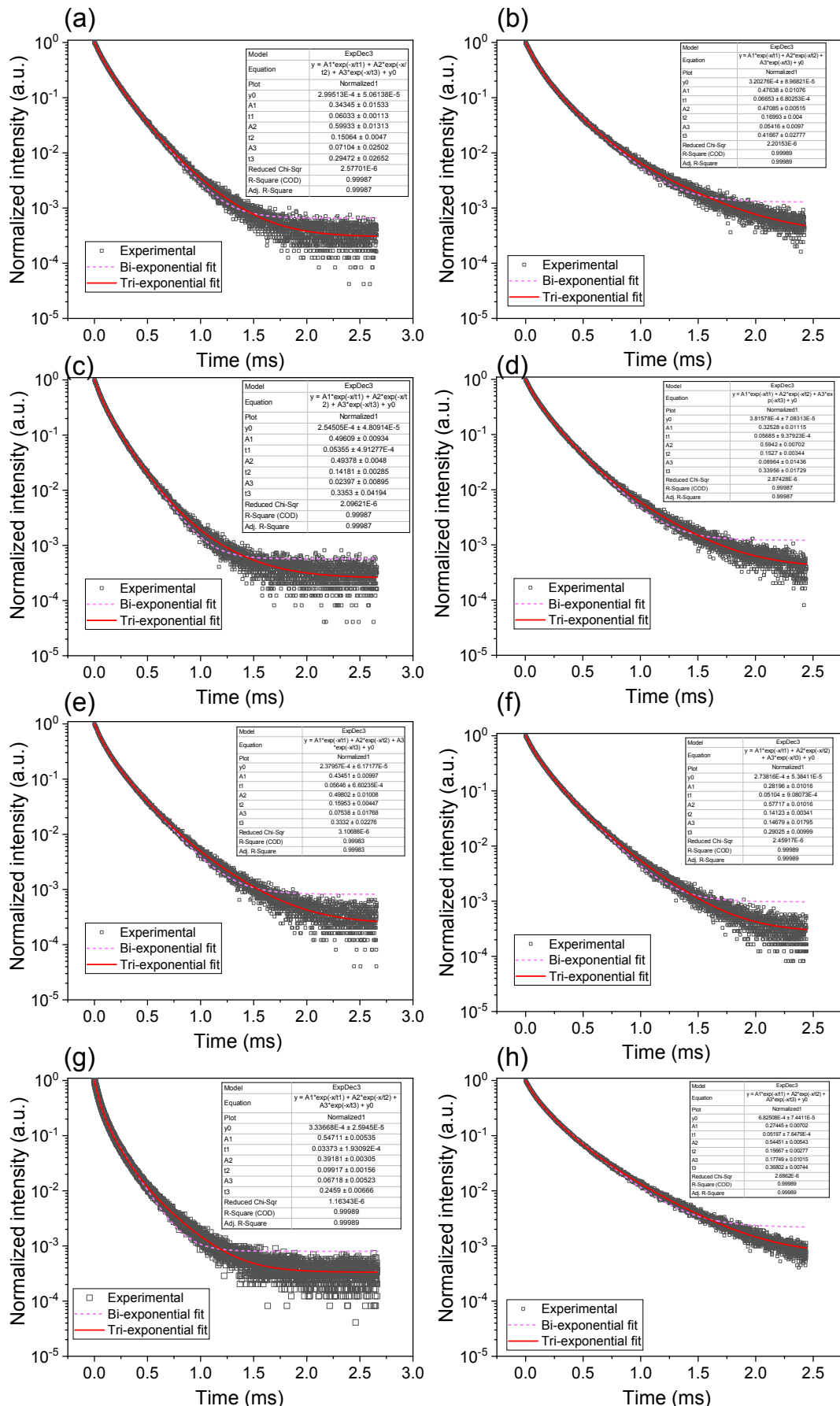


**Fig S22.** Luminescence lifetimes ( ${}^5D_0$ ) in (a,c,e,g)  $H_2O$  or (b,d,f,h)  $D_2O$  of  $(Y_{0.60}Eu_{0.40})VO_4$  nanoparticles prepared by one-pot conversion of hydroxycarbonates in different  $H_2O/EG$  (vol/vol) solvent conditions, namely (a,b) 3/2, (c,d) 1/1, (e,f) 1/2, (g,h) 1/3.

## 2.12. Spectroscopic Parameters

**Table S4.** Eu<sup>3+</sup> spectroscopic parameters (<sup>5</sup>D<sub>0</sub> level) calculated from emission spectra (Fig. 7) and decay curves (Fig. S19-S21) of the (Y,Eu)VO<sub>4</sub> nanoparticles prepared by one-pot conversion of RE hydroxycarbonates in different water/EG volume ratios (3/2, 1/1, 1/2, 1/3) as suspensions in H<sub>2</sub>O or D<sub>2</sub>O: pre-exponential factors (A<sub>1</sub>, A<sub>2</sub>, A<sub>3</sub>) and lifetimes (τ<sub>1</sub>, τ<sub>2</sub>, τ<sub>3</sub>) calculated from fitting of luminescence decay curves, average luminescence lifetimes (τ<sub>av</sub>), radiative (A<sub>RAD</sub>) and non-radiative (A<sub>NRAD</sub>) decay rates, internal quantum yields (η), and overall quantum yields under λ<sub>exc</sub>=280 nm (q<sub>EXP</sub>)

H <sub>2</sub> O/EG (v/v)	A <sub>1</sub>	τ <sub>1</sub> (ms)	A <sub>2</sub>	τ <sub>2</sub> (ms)	A <sub>3</sub>	τ <sub>3</sub> (ms)	τ <sub>av</sub> (ms)	A <sub>RAD</sub> (s <sup>-1</sup> )	A <sub>NRAD</sub> (s <sup>-1</sup> )	η (%)	q <sub>EXP</sub> (%)
<b>Y<sub>0.95</sub>Eu<sub>0.05</sub>VO<sub>4</sub></b>											
3/2	0.11	0.11	0.46	0.40	0.42	0.87	0.70	428	1005	29.8	--
1/1	0.21	0.10	0.50	0.37	0.36	0.82	0.63	438	1161	27.4	--
1/2	0.18	0.09	0.45	0.35	0.38	0.80	0.63	428	1154	27.1	--
1/3	0.18	0.10	0.45	0.39	0.36	1.03	0.80	434	821	34.6	--
<b>Y<sub>0.80</sub>Eu<sub>0.20</sub>VO<sub>4</sub></b>											
3/2	0.14	0.08	0.41	0.28	0.46	0.55	0.45	484	1733	21.8	3.6
1/1	0.25	0.08	0.51	0.25	0.25	0.49	0.35	474	2424	16.3	2.5
1/2	0.31	0.07	0.48	0.22	0.23	0.47	0.32	459	2670	14.7	1.8
1/3	0.26	0.05	0.46	0.19	0.30	0.46	0.34	467	2508	15.7	1.9
<b>Y<sub>0.60</sub>Eu<sub>0.40</sub>VO<sub>4</sub></b>											
3/2	0.34	0.06	0.60	0.15	0.07	0.29	0.16	462	5815	7.4	--
1/1	0.50	0.05	0.49	0.14	0.02	0.34	0.13	457	6991	6.1	--
1/2	0.43	0.06	0.50	0.16	0.08	0.33	0.17	445	5311	7.7	--
1/3	0.55	0.03	0.39	0.10	0.07	0.25	0.12	448	8201	5.2	--

Table S4. (cont.)

H <sub>2</sub> O/EG (v/v)	A <sub>1</sub>	τ <sub>1</sub> (ms)	A <sub>2</sub>	τ <sub>2</sub> (ms)	A <sub>3</sub>	τ <sub>3</sub> (ms)	τ <sub>av</sub> (ms)	A <sub>RAD</sub> (s <sup>-1</sup> )	A <sub>NRAD</sub> (s <sup>-1</sup> )	η (%)	q <sub>EXP</sub> (%)
<i>Y<sub>0.95</sub>Eu<sub>0.05</sub>VO<sub>4</sub> in D<sub>2</sub>O</i>											
3/2	0.09	0.15	0.31	0.64	0.60	1.25	1.11	477	426	52.9	--
1/1	0.14	0.10	0.39	0.42	0.46	1.02	0.85	470	710	39.8	--
1/2	0.26	0.09	0.41	0.35	0.34	1.00	0.77	450	852	34.6	--
1/3	0.10	0.14	0.36	0.65	0.54	1.35	1.17	441	414	51.6	--
<i>Y<sub>0.80</sub>Eu<sub>0.20</sub>VO<sub>4</sub> in D<sub>2</sub>O</i>											
3/2	0.25	0.07	0.47	0.27	0.29	0.69	0.50	475	1524	23.8	5.2
1/1	0.23	0.09	0.43	0.34	0.35	0.81	0.62	490	1117	30.5	3.8
1/2	0.11	0.08	0.31	0.39	0.58	0.94	0.83	467	732	38.9	4.6
1/3	0.30	0.06	0.47	0.26	0.24	0.77	0.54	443	1407	24.0	3.7
<i>Y<sub>0.60</sub>Eu<sub>0.40</sub>VO<sub>4</sub> in D<sub>2</sub>O</i>											
3/2	0.48	0.07	0.47	0.17	0.05	0.42	0.19	447	4901	8.4	--
1/1	0.33	0.06	0.59	0.15	0.09	0.34	0.18	452	5081	8.2	--
1/2	0.28	0.05	0.58	0.14	0.15	0.29	0.18	456	5171	8.1	--
1/3	0.27	0.05	0.54	0.16	0.18	0.37	0.23	451	3872	10.4	--

### 3. REFERENCES

1. Zhang, F.; Ilavsky, J.; Long, G.; Quintana, J.; Allen, A.; Jemian, P. Glassy Carbon as an Absolute Intensity Calibration Standard for Small-Angle Scattering. *Metal. Mater. Trans A* **2010**, 41, 1151-1158.
2. Ilvasky, J.; Jemain, P.R. Irena: Tool Suite for Modeling and Analysis of Small-Angle Scattering. *J. Appl. Cryst.* **2009**, 42, 347-353.
3. Rusakowicz, R.; Testa, A. C. 2-Aminopyridine as a Standard for Low-Wavelength Spectrofluorimetry. *J. Phys. Chem.* **1968**, 72, 2680–2681.
4. de Sousa Filho, P.C.; Larquet, E.; Dragoe, D.; Serra, O.A.; Gacoin, T. Lanthanoid-Doped Phosphate/Vanadate Mixed Hollow Particles as Ratiometric Luminescent Sensors. *ACS Appl. Mater. Interfaces* **2017**, 9, 1635-1644
5. Breßler, I.; Kohlbrecher, J.; Thünemann, A. F.; SASfit: A Tool for Small-Angle Scattering Data Analysis Using a Library of Analytical Expressions. *J. Appl. Cryst.* **2015**, 48, 1587-1598.
6. Bohne, D.; Fischer, S.; Obermeier, E. Thermal Conductivity, Density, Viscosity, and Prandtl-Numbers of Ethylene Glycol-Water Mixtures. *Ber. Bunsen. Phys. Chem.* **1984**, 88, 739-742.